A p53-responsive microRNA network promotes cancer cell quiescence

Ting La,[1] Guang Zhi Liu,[2] Margaret Farrelly,[1] Nicole Cole,[3] Yu Chen Feng,[1] Yuan Yuan Zhang,[1] Simonne K. Sherwin,[1] Hamed Yari,[1] Hessam Tabatabaee,[1] Xu Guang Yan,[1] Su Tang Guo,[4] Tao Liu,[5] Rick F. Thorne, [2,6] Lei Jin,[7]* Xu Dong Zhang[1,2]*

[1]School of Biomedical Sciences and Pharmacy, The University of Newcastle, NSW, 2308, Australia

[2]Translational Research Institute, Henan Provincial People's Hospital, Academy of Medical Science, Zhengzhou University, Henan, 450053, China

[3]Research Infrastructure, Research and Innovation Division, The University of Newcastle, NSW, 2308, Australia

[4]Department of Molecular Biology, Shanxi Cancer Hospital and Institute, Shanxi, 030013, China

[5]Children's Cancer Institute Australia for Medical Research, University of New South Wales, NSW 2750, Australia

[6]School of Environmental and Life Sciences, University of Newcastle, NSW 2308, Australia

[7]School of Medicine and Public Health, The University of Newcastle, NSW, 2308, Australia

Running title: p53 regulates quiescence via microRNAs

*Correspondence: Lei Jin or Xu Dong Zhang, LS3-49, Life Science Building, University of Newcastle, Callaghan, NSW, Australia.

Ph: 61 2 49218906. Fax: 61 2 49217311.

Email: Lei.Jin@newcastle.edu.au or Xu.Zhang@newcastle.edu.au

The authors state no conflict of interest.

ABSTRACT

Cancer cells in quiescence (G0 phase) are resistant to death, and re-entry of quiescent cancer cells into the cell cycle plays an important role in cancer recurrence. Here we show that two p53-responsive microRNAs (miRNAs) utilize distinct but complementary mechanisms to promote cancer cell quiescence by facilitating stabilization of p27. Purified quiescent B16 mouse melanoma cells expressed higher levels of miRNA-27b-3p and miRNA-455-3p relative to their proliferating counterparts. Induction of quiescence resulted in increased levels of these miRNAs in diverse types of human cancer cell lines. Inhibition of miRNA-27b-3p or miRNA-455-3p reduced, whereas its overexpression increased, the proportion of quiescent cells in the population, indicating that these miRNAs promote cancer cell quiescence. Accordingly, cancer xenografts bearing miRNA-27b-3p or miRNA-455-3p mimics were retarded in growth. miRNA-27b-3p targeted cyclin-dependent kinase regulatory subunit 1 (CKS1B), leading to reduction in p27 polyubiquitination mediated by S-phase kinase-associated protein 2 (Skp2). miRNA-455-3p targeted CDK2-associated cullin domain 1 (CACUL1), which enhanced CDK2-mediated phosphorylation of p27 necessary for its polyubiquitination. Of note, the gene encoding miRNA-27b-3p was embedded in the intron of the chromosome 9 open reading frame 3 gene that was transcriptionally activated by p53. Similarly, the host gene of miRNA-455-3p, collagen alpha-1 chain, was also a p53 transcriptional target. Collectively, our results identify miRNA-27b-3p and miRNA-455-3p as important regulators of cancer cell quiescence in response to p53 and suggest that manipulating miRNA-27b-3p and miRNA-455-3p may constitute novel therapeutic avenues for improving outcomes of cancer treatment.

INTRODUCTION

Despite the advance in cancer treatment using molecularly targeted therapies and resurgence of immunotherapy, relapse following initial disease remission remains an unsolved problem (1). Recurrent and metastatic cancer lesions often undergo a period of dormancy (2), which can be conceptually classified into two models (3). The first is tumour mass dormancy whereby the rate of tumour cell proliferation is balanced by the rate of programmed cell death, mostly apoptosis, caused by the lack of vasculature (angiogenic dormancy) and/or anti-cancer immune responses (immunologic dormancy) (3) . The second is cellular dormancy resulting from cell-intrinsic or extrinsic mechanisms leading to a state of quiescence where cells exit the cell cycle and are reversibly arrested in G0 phase. These models are not mutually exclusive. In particular, it is cellular dormancy that renders cancer cells fundamentally resistant to cell death and refractory to therapeutics (3). Consequently, curative cancer treatment requires therapies that either sustain the dormant state or effectively kill quiescent cancer cells.

Molecular signatures of cellular quiescence in some types of cells, such as hematopoietic stem cells and fibroblasts have been documented (4,5). Although changes in gene expression/activation vary depending on cell type and context, quiescent cells generally display reduction in the expression of pro-proliferation genes and upregulation of genes encoding cyclin-dependent kinase (CDK) inhibitors and those associated with remodeling the extracellular environment (6,7). A variety of signal pathways, such as the MEK/ERK and p38 pathways contribute to regulation of cellular quiescence in cancer (8). These pathways commonly converge on modulation of the Rb-E2F bistable switch that is a master regulator of cell cycle progression (9). Noticeably, the tumor suppressor p53 also plays a role in regulating quiescence, but the mechanisms involved remain to be fully understood (10).

Here we demonstrate that p53 promotes cancer cell quiescence through a miRNA network encompassing miRNA-27b-3p and miRNA-455-3p. While miRNA-27b-3p targets cyclin-dependent kinases regulatory subunit 1 (Cks1), a cofactor of S-phase kinase-associated protein 2 (Skp2) that is important for p27 polyubiquitination and subsequent degradation (11), miRNA-455-3p targets CDK2

associated cullin domain 1 (CAC1) that promotes the kinase activity of CDK2 leading to phosphorylation of p27 for Skp2-mediated polyubiquitination (12,13). Thus, the manipulation of miRNA-27b-3p and miRNA-455-3p to maintain or disrupt cancer cell quiescence may provide potential avenues to improve the therapeutic efficacy of systemic cancer treatments.

MATERIALS AND METHODS

Cell culture

The human melanoma cell lines Mel-RM, Sk-Mel-28, A375 and mouse melanoma cell line B16 were cultured in DMEM containing 5% FCS (14). HEK293T, A549, MCF7, HeLa, WiDr, HT29, HCT116, U2OS cells were obtained from ATCC and cultured according to ATCC instructions. All cell lines were verified to be free of mycoplasma contamination every 3 months and were authenticated by short tandem repeat (STR) profiling in April 2018 by Australian Genome Research Facility (AGRF). The passage numbers of all the cell lines used in this paper are less than 30 after thawing.

Antibodies and reagents

Information on antibodies and reagents used in this study is provided in Supplementary Table 1 & 2.

Small interference RNA (siRNA) and short hairpin RNA (shRNA)

siRNAs were obtained from GenePharma (Shanghai, China) and transfected using Lipofectamine 2000 reagent (Invitrogen). The human control and CDKN1A MISSION® shRNA lentiviral transduction particles were purchased from Sigma-Aldrich (Castle Hill, NSW, Australia). Lentiviral particle transduction was carried out as per the manufacturer's protocols. The siRNA and shRNA sequences were listed in Supplementary Table 3.

Plasmids

pMXs-IP-mVenus-p27K$^-$, pGag-pol-IRES-bs^r and pEnv-IRES-puro^r were generous gifts from professor Toshio Kitamura (University of Tokyo, Tokyo, Japan). mCherry-hCdt1(30/120)/ pCSII-EF-MCS was generous gift from Dr. Hiroyuki Miyoshi and Dr.Atsushi Miyawaki (RIKEN Brain Science Institute, Japan). Other plasmids used are detailed in Supplementary Table 4 & 5.

miRNA profiling and Real-time PCR

Total RNA was isolated using the ISOLATE II RNA Mini Kit (Bioline) according to manufacturer's protocols. RNA sequencing (10M 50SE) was performed to characterize miRNA expression profiles (BGI, Hong Kong). The results have been deposited to the Gene Expression Omnibus (GEO) (GEO accession: GSE118547).

Reverse transcription was undertaken using the qScript cDNA Supermix (Quantabio, 95048) and TaqMan™ MicroRNA Reverse Transcription Kit (ThermoFish Scientific, 4366596) for mRNAs and miRNAs, respectively. qPCR was performed with 20 µl reaction volume using SensiFAST™ SYBR Hi-ROX Kit (Bioline). The 2-ΔΔCT method was applied to calculate the relative expression levels of genes. Primers used are detailed in Supplementary Table 6.

Western blotting and Immunoprecipitation (IP)

Western blotting and IP were carried out as described in previous publication (14). The relative intensity of bands was quantified using Image J and normalized against GAPDH.

Serum starvation and contact inhibition

Cell confluence was monitored until the control group reached 70-80% confluence. For serum starvation, cell culture medium was replaced with serum-free medium. For serum replenishment, serum-free medium was replaced by medium containing 5% FCS. For contact inhibition, culture medium was refreshed every 24 hours after cells reached 100% confluence.

G0 and G1 cell isolation

pMXs-IP-mVenus-p27K$^-$,pGag-pol-IRES-bs^r and pEnv-IRES-puro^r were used to package retrovirus to deliver mVenus-p27K$^-$, whereas pMDLg.pRRE, pRSU.pREV, pMD2.g and mCherry-hCdt1(30-120) pCSII-EF-MCS were used to package lentivirus to deliver mCherry-hCdt1(30-120) into cells. Cells were transduced with viral particles carrying mCherry-hCdt1(30-120) and the mCherry-positive cells isolated by FACS were further transduced with viral particles carrying mVenus-p27K$^-$. Cells positive for both mVenus-p27K$^-$ and mCherry-hCdt1(30-120) were selected by the addition of puromycin (3

μg/ml). G0 cells (mVenus-p27K^{-high}/mCherry-hCDT1(30/120)$^{+}$) and G1 cells (mVenus-p27K^{-low}/mCherry-hCDT1(30/120)$^{+}$) were isolated using FACS sorting (FACSAria III, BD).

Cell cycle analysis

For Ki67/DNA double staining, cells fixed with cold 70% ethanol at -20 °C for 2 hours were washed with staining buffer (BioLegend, #420201) for three times before stained with APC-conjugated anti-Ki-67 antibody (BioLegend, #652406). After washing, cells were suspended in PI staining buffer and analysed using a flow cytometer (FACSCanto II, BD). Hoechst 33342/Pyronin Y double staining were carried according to protocols described previously (15). In brief, cells were stained with 2 μg/ml Hoechst 33258 for 45 minutes and 4 μg/ml Pyronin Y for additional 15 minutes. DNA and RNA contents were determined using a flow cytometer (LSRFORTESSA X-20, BD).

Clonogenic assay

Cells were seeded in six-well plates at 1000 cells/well. About two weeks later, cells were stained with crystal violet (0.5%). ColonyArea was quantitated using ImageJ-plugin. ColonyArea in cells introduced with Ctrl mimics was arbitrarily designated as 1.

Luciferase reporter assay

Reporter activities were measured as per the manufacturer's protocol (Dual-Glo® Luciferase Assay System, Promega). Briefly, psiCHECK-2 vector-based plasmids were co-transfected with miRNA mimics or anti-miRNAs into cells. Alternatively pGL3-basic vector-based plasmids were co-transfected with pRL-SV40P. Firefly and Renilla luciferase activities were recorded using a microplate reader (BioTek, VT).

Chromatin Immunoprecipitation (ChIP) assay

Cells were harvested and subjected to ChIP assays according to the manufacturer's protocol (MAGnify™ Chromatin Immunoprecipitation System, ThermoFisher Scientific, 49-2024). PCR products were separated by gel electrophoresis on 2% agarose gel.

Senescence

Senescence was detected by staining senescence-associated (SA) β-galactosidase (β-gal) using a Senescence Detection Kit (Sigma-Aldrich, CS0030-1KT). Briefly, cells were washed twice and then fixed at room temperature. After washing, cells were stained with a staining mixture. Slides were then examined using a light microscope and SA-β-gal positive cells were calculated across 5 random high-power fields.

Apoptosis

Apoptotic cells were quantitated using the Annexin V/Propidium Iodide (PI) Apoptosis Detection Kit (BD Biosciences). In brief, cells in binding buffer were incubated with Annexin V/PI for 15 min before analysis using a flow cytometer (FACSCanto II, BD Biosciences).

Xenograft mouse model

The animal experiments were conducted as our previously described with approval from the Animal Research Ethics Committee of Shanxi Cancer Hospital of China (16). Briefly, male BALB/c nude mice (4-week old; Model Animal Research Centre of Nanjing University, China) were subcutaneously injected with Mel-RM cells with or without stable overexpression of miR-27b-3p or miR-455-3p (1×10^7). Each groups contained 6 mice. Tumour growth was monitored using a calliper.

Statistical analysis

Statistical analysis was carried out using GraphPad Prism 7. Statistical significance was analysed by Student's *t*-test and expressed as a P value. $P < 0.05$ were considered to be statistical significance.

RESULTS

MiR-27b-3p and miR-455-3p promote cellular quiescence

To isolate cancer cells in the quiescent (G0) state, we employed a model system encompassing an mVenus-tagged p27 deletion mutant lacking the CDK-binding domain (mVenus-p27K$^-$) together with a mCherry-tagged truncated mutant of human chromatin licensing and DNA replication factor 1 (hCDT1) (mCherry-hCDT1(30/120)) (17). While hCDT1 is exclusively expressed in cells in G0 and G1 phases, p27 is markedly more abundant in G0 compared with G1 cells (18,19). After co-introduction of these constructs into B16 mouse melanoma cells, distinctive populations of mVenus-p27K^{-low} and mVenus-p27K^{-high} cells positive for mCherry-hCDT1(30/120) were observed (Fig. 1A). The population of mVenus-p27K^{-high} mCherry-hCDT1(30/120)$^+$ cells was enriched by serum starvation or contact inhibition (Fig. 1A and Fig. 1B), suggesting that this population represented cells in the quiescent state (20). In support, mVenus-p27K^{-high} mCherry-hCDT1(30/120)$^+$ cells displayed typical G0 features including substantially higher levels of endogenous p27 and p21, but with low Ki67 expression and reduced levels of phosphorylated retinoblastoma protein (pRb), cyclin D1 and cyclin-dependent kinase 2 (CDK2) compared with mVenus-p27K^{-low} mCherry-hCDT1(30/120)$^+$ cells (Fig. 1C and D). Moreover, dual nucleic acid staining (DNA stained with Hoechst-33342, and RNA with Pyronin Y) identified these cells to be diploid with low RNA content (Fig. 1E), characteristic of cells in the quiescent state (21).

We then undertook a comparative analysis of miRNA expression profiles between G0 (mVenus-p27K^{-high} mCherry-hCDT1(30/120)$^+$) and G1 (mVenus-p27K^{-low} mCherry-hCDT1(30/120)$^+$) cells isolated using FACS (Fig. 1A). Comparing RNA sequencing (RNA-seq) data we derived a list of differentially expressed miRNAs (Supplementary Table 7). Focussing on the most prominently upregulated miRNAs in G0 cells, we confirmed that four of the five candidate miRNAs were significantly increased in G0 compared to G1 cells using qPCR (Fig. 1F). As anticipated, the expression of these miRNAs was also increased in the total unfractionated population of B16 cells,

albeit to a lesser extent, under serum starvation or contact inhibition conditions (Supplementary Fig. 1A).

Strikingly, inhibition of miRNA-27b-3p or miRNA-455-3p but not inhibition of the other miRNAs diminished the induction of quiescence (Fig. 1G & H and supplementary Fig. 1B-D). In contrast, introduction of miRNA-27b-3p or miRNA-455-3p mimics increased the proportion of cells in G0 phase (Fig. 1I & J and supplementary Fig. 1E - G). Of note, neither inhibition of miRNA-27b-3p or miRNA-455-3p nor introduction of its mimics triggered cellular senescence or apoptosis (Supplementary Fig. 1H & I). Moreover, no additive or synergistic effects on quiescence were observed when both miRNAs were co-manipulated (Fig. 1H & J), suggesting that these miRNAs might be functionally interrelated.

Both miRNA-27b-3p and miRNA-455-3p are highly conserved among mammalian species (Supplementary Fig. 2), proposing that their biological functions may also be broadly preserved. Indeed, serum starvation similarly increased the levels of these miRNAs in a range of human cancer cell lines, Mel-RM (melanoma), U2OS (osteosarcoma), A549 (lung) and HCT116 (colon), which were reduced to the basal levels after serum replenishment (Fig. 2A). Moreover, introduction of anti-miRNA-27b-3p or anti-miRNA-455-3p blunted the induction of quiescence (Fig. 2B). This was associated with inhibition of upregulation of p27 and downregulation of Ki67, pRB, cyclin D1 and CDK2 (Fig. 2C & D). Conversely, introduction of miRNA-27b-3p or miRNA-455-3p mimics promoted quiescence along with upregulation of p27 and reduction in Ki67, pRB, cyclin D1 and CDK2 expression (Fig. 2E - G). Noticeably, manipulation of miRNA-27b-3p or anti-miRNA-455-3p did not affect the upregulation of p21 caused serum starvation (Fig. 2C & F), suggesting that p21 upregulation in quiescent cells was not associated with these miRNAs. In accordance with induction of cellular quiescence, both miRNA-27b-3p and miRNA-455-3p negatively regulated cell proliferation and clonogenicity (Fig. 2H & I). This was mirrored *in vivo* when Mel-RM cells bearing miRNA-27b-3p or miRNA-455-3p mimics were transplanted into nu/nu mice (Fig. 2J). Taken together, these results identified miRNA-27b-3p and miRNA-455-3p as facilitators of cancer cell quiescence.

MiR-27b-3p and miR-455-3p promote p27 stabilization through downregulating Skp2 and promoting its phosphorylation at Thr187, respectively

We investigated how miRNA-27b-3p and miRNA-455-3p affect p27 expression that is essential for cellular quiescence (22). Inhibition of either miRNA accelerated the turnover rate of the p27 protein (Fig. 3A), whereas introduction of miRNA-27b-3p or miRNA-455-3p mimics prolonged its half-life time (Supplementary Fig. 3A). These manipulations did not influence the expression of p27 mRNA (Supplementary Fig. 3B). Rather, inhibition of miR-27b-3p or miR-455-3p was associated with increased p27 polyubiquitination (Fig 3B & Supplementary Fig. 3C). This infers that the p27 upregulation caused by miRNA-27b-3p and miRNA-455-3p is associated with inhibition of p27 polyubiquitination that prevents its degradation (23).

Interestingly, inhibition of miRNA-27b-3p but not miRNA-455-3p prolonged the half-life time of the Skp2 protein, whereases introduction of miRNA-27b-3p mimics accelerated Skp2 protein turnover rate (Fig. 3C and Supplementary Fig. 3D), suggesting that posttranslational regulation of p27 by miRNA-27b-3p may involve Skp2. Indeed, knockdown of Skp2 counteracted the accelerated p27 turnover associated with inhibition of miRNA-27b-3p (Fig. 3D), whereas overexpression of Skp2 abolished the prolonged p27 half-life time triggered by miRNA-27b-3p mimics (Supplementary Fig. 3E). These results consolidated the functional association between miRNA-27b-3p and Skp2-mediated regulation of p27. Intriguingly, Skp2 knockdown and overexpression also diminished the changes in the p27 turnover rate caused by anti-miRNA-455-3p and miRNA-455-3p mimics, respectively (Fig. 3E and Supplementary Fig. 3F), suggesting that miRNA-455-3p-mediated promotion of p27 stabilization also requires Skp2.

Since p27 phosphorylation at Thr187 is necessary for Skp2-mediated polyubiquitination (23), we examined whether miRNA-455-3p affects phosphorylation of p27. Introduction of anti-miRNA-455-3p but not anti-miRNA-27b-3p enhanced Thr187 phosphorylation of p27, which was associated with a decrease in p27 expression (Fig. 3F). In contrast, introduction of miRNA-455-3p mimics reduced p27 phosphorylation at Thr187 (Fig. 3G). Neither anti-miRNA-455-3p nor miRNA-455-3p mimics altered

the p27 phosphorylation at Ser10 or Thr198 (Fig. 3F & G), suggesting that regulation of p27 phosphorylation at Thr187 by miRNA-455-3p is specific. In support, a point mutation of Thr187 disabled the ability of miRNA-455-3p to regulate p27 phosphorylation and its turnover rate (Fig. 3H and Supplementary Fig 3G & H). Therefore, miRNA-455-3p promotes p27 stability through inhibiting its phosphorylation at Thr187.

MiR-27b-3p suppresses Skp2 expression through targeting Cks1, whereas miR-455-3p inhibits p27 phosphorylation through targeting CAC1

In silico analysis showed that amongst predicted targets of miRNA-27b-3p was Cks1, a cofactor of Skp2 that prevents Skp2 auto-ubiquitylation and degradation (Supplementary Fig. 4A) (24). To test whether Cks1 3′UTR is targeted by miRNA-27b-3p, we introduced luciferase reporter plasmids containing the 3′UTR of Cks1 into Mel-RM and A549 cells (Supplementary Fig. 4B). The reporter activity was reduced, albeit moderately, by the presence of the 3′UTR of Cks1, which was reversed when the 3′UTR was mutated (Fig. 4A), indicating that the 3′UTR of Cks1 was inhibited by endogenous miRNA-27b-3p. In support, co-introduction of anti-miRNA-27b-3p increased, whereas co-introduction of miRNA-27b-3p mimics further reduced the reporter activity (Fig. 4A & B). Therefore, miRNA-27b-3p targets the 3′UTR of Cks1. Consistently, introduction of miRNA-27b-3p mimics into Mel-RM and A549 cells down-regulated the levels of endogenous Cks1, whereas introduction of anti-miRNA-27b-3p increased Cks1 expression levels (Fig. 4C & D). Moreover, the decreased Skp2 expression in cells treated with miRNA-27b-3p mimics was reversed by overexpression of Cks1 and conversely, the increase Skp2 expression caused by anti-miRNA-27b-3p was abolished by Cks1 knockdown (Fig. 4E & F). Further supporting the regulatory effect of miRNA-27b-3p on Cks1, the levels of miRNA-27b-3p were inversely correlated with Cks1 protein expression levels (Supplementary Fig. 4C & D).

Interrogation of potential targets of miRNA-455-3p highlighted CAC1 (Supplementary Fig. 4E), known to promote the kinase activity of CDK2 (12). Similar to experiments undertaken with miRNA-27b-3p, we introduced luciferase reporter plasmids of the 3′UTR of CAC1 into Mel-RM and A549

cells (Supplementary Fig. 4B). The reporter activity was reduced by the presence of the 3′UTR but this was abolished when the 3′UTR was mutated (Fig. 4G). Moreover, co-introduction of anti-miRNA-455-3p promoted, whereas co-introduction of miRNA-455-3p mimics further inhibited the reporter activity (Fig. 4G & H). In accordance, miRNA-455-3p mimics reduced, whereas anti-miRNA-455-3p upregulated endogenous expression of CAC1 (Fig. 4I & J). Therefore, miRNA-455-3p targets the 3′UTR of CAC1. Consistently, co-introduction of miRNA-455-3p mimics reversed the CAC overexpression-triggered enhancement in the kinase activity of CDK2 and phosphorylation of p27 at Thr187 (Fig. 4K). In contrast, antagonising miRNA-455-3p increased CDK2 activity and Thr187-phosphorylated p27, which was diminished by knockdown of CAC1 (Fig, 4L). Taken together, these results indicate that miRNA-455-3p targets the 3′UTR of CAC1 to attenuate CDK2 activity and thus prevent Thr187 phosphorylation of p27 (13). Indeed, the expression levels of miRNA-455-3p were inversely correlated with CAC1 protein expression levels (Supplementary Fig. 4C & F).

Co-regulation of miRNA-27b-3p and miRNA-455-3p and their host genes

The pre-miRNA-27b-3p is embedded within the last intron of the human *Chromosome 9 open reading frame 3* (*C9ORF3*) gene, whereas the pre-miRNA-455-3p is located to the tenth intron of the human *collagen alpha-1 (XXVII) chain* (*COL27A1*) gene (Supplementary Fig. 5). Intriguingly, analysis of publicly available expression profiles in 35,763 of cancers of diverse types acquired from the R2 Genomics Analysis and Visualization Platform revealed that *C9ORF3* and *COL27A1* mRNA expression levels were positively correlated (Fig. 5A) (R2: http://r2.amc.nl), consistent with the relationship between the expression of miRNA-27b-3p and miRNA-455-3p in a panel of human cancer cell lines (Fig. 5B). Indeed, knockdown of *C9ORF3* and *COL27A1* inhibited the expression of miRNA-27b-3p and miRNA-455-3p, respectively (Fig. 5C & D). In support, both *C9ORF3* and *COL27A1* were upregulated by serum starvation and this upregulation was diminished after serum replenishment (Fig. 5E). Moreover, knockdown of *C9ORF3* or *COL27A1* diminished induction of quiescence by serum starvation (Fig. 5F). These observations suggest that transcriptional regulation of *C9ORF*3 or *COL27A1* expression may potentially be controlled though a common mechanism.

p53 transcriptionally regulates miRNA-27b-3p and miRNA-455-3p

Luciferase reporter assays using constructs having incremental deletions spanning ~1500 bases upstream down to 100 bp downstream of the *C9ORF*3 gene transcription start site showed that the -250 ~ -100 segment was the shortest region that remained active in Mel-RM cells undergoing serum starvation (Fig. 6A). By use of the same approach, the -1000 ~ -500 fragment was identified to be the shortest region of the *COL27A1* gene that remained transcriptionally active in in serum-starved cells (Fig. 6B). Importantly, serum replenishment decreased the transcriptional activities of the -250 ~ -100 segment of the *C9ORF*3 gene and the -1000 ~ -500 fragment of the *COL27A1* gene (Fig. 6C & D), confirming that these genes are transcriptionally responsive to serum starvation.

Examination of the minimally active promoter regions of both genes showed that they shared in common consensus binding sites for p53 (Supplementary Fig. 6A). One putative p53 binding site (p53-BS) (-157 to -143 bp) was identified at the -250 ~ -100 segment of the *C9ORF*3 gene whereas the -1000 ~ -500 segment of the *COL27A1* gene also contained three consensus p53-BSs (-929 to -915 bp, -919 to -905 bp and -814 to -800 bp) (Supplementary Fig. 6A). Deletion of the p53-BS in the *C9ORF*3 reporter construct diminished its transcriptional activity (Fig. 6E), whereas deletion of the p53-BSs in the *COL27A1* construct similarly abolished its transcriptional activity (Fig. 6F), indicating that the p53-BSs were responsible for the increased transcriptional activity in response to serum starvation.

Further reporter assay experiments showed that enforced overexpression of wild-type p53 enhanced the reporter activity of both *C9ORF*3 and *COL27A1* reporters while the p53ΔTA mutant (lacking the transactivation domain) did not augment transcription (Fig. 6G). In addition, knockdown of p53 or treatment with the small molecule inhibitor of p53 transcriptional activity, pifithrin-α (PFT-α), inhibited activation of the p53-BS-containing luciferase reporters of both genes (Fig. 6H & I), confirming that the response of the p53-BSs to induction of quiescence is mediated by p53. This was supported by binding of p53 to the p53-BSs at both genes, which was enhanced by serum starvation (Fig. 6J). Therefore, the putative p53-BSs are responsive to p53 that was increased upon induction of

quiescence (Supplementary Fig. 6A) (25). In accordance, p53 knockdown or treatment with PFT-α reduced the endogenous expression levels of *C9ORF3* and *COL27A1* (Supplementary Fig. 6B & C).

We tested whether p53 is similarly important for miRNA-27b-3p and miRNA-455-3p expression. Since p53 is also essential for miRNA processing (26), we examined its effect on the expression of pri-miRNA-27b-3p and pri-miRNA-455-3p. Knockdown of p53 or treatment with PFT-α downregulated pri-miRNA-27b-3p and pri-miRNA-455-3p and abolished their upregulation in response to serum starvation (Fig. 6K and L). Conversely, overexpression of p53 promoted the expression of these pri-miRNAs in cells with or without serum starvation or contact inhibition (Fig. 6M). Therefore, binding of p53 to the p53-BSs at the *C9ORF3* and *COL27A1* gene transcriptionally upregulates miRNA-27b-3p and miRNA-455-3p in response to induction of cellular quiescence. Of note, although the expression levels of miRNA-27b-3p and miRNA-455-3p and their host genes appeared to correlate with wild-type p53 protein expression in cancer cell lines (Supplementary Fig. 6D &E), analysis of publicly available datasets acquired from the TCGA did not show any significant relationship between the expression levels of these miRNAs and the *TP53* mutational status or wild-type p53 mRNA expression levels (Supplementary Fig. 6F & G).

p53 drives cellular quiescence through miRNA-27b-3p and miRNA-455-3p

Knockdown of p53 reduced the proportion of quiescent cells, phenocopying introduction of anti-miRNA-27b-3p or anti-miRNA-455-3p (Fig. 2B & Supplementary Fig. 7A). In contrast, overexpression of p53 promoted quiescence, similar to introduction of miRNA-27b-3p or miRNA-455-3p mimics (Fig. 2E & Supplementary Fig. 7B). Co-introduction of miRNA-27b-3p or miRNA-455-3p mimics reversed the reduction in quiescence caused by p53 knocked down, whereas co-introduction of anti-miRNA-27b-3p or anti-miRNA-455-3p blocked promotion of quiescence by overexpression of p53 (Fig. 7A & B), confirming that p53-induced cellular quiescence is mediated through these miRNAs. Similar to p53, the *C9ORF3* and *COL27A1* genes appeared to play a role in regulating cellular quiescence through miRNA-27b-3p and miRNA-455-3p, respectively (Supplementary Fig. 7C & D).

Knockdown of p53 also resulted in downregulation of p27 that was associated with shortened half-life of the protein, whereas overexpression of p53 increased p27 expression in association with prolonging its half-life (Supplementary Fig. 7E & F). The effect of p53 knockdown on p27 expression was diminished by co-introduction of miRNA-27b-3p or miRNA-455-3p mimics (Fig. 7C). Consistently, the effect of p53 overexpression on p27 expression was reduced by co-introduction of anti-miRNA-27b-3p or anti- miRNA-455-3p (Fig. 7D). These results further consolidate that p53 promotes p27 stability through these miRNAs. Knockdown of p27 diminished p53-overexpression-casued promotion of cellular quiescence (Fig. 7E), whereas overexpression of p27 increased the G0 cell proportion irrespective of the p53 expression status (Fig. 7F), indicating that upregulation of p27 is necessary for p53-mediated cellular quiescence. Of note, p21 which plays an important role in p53-mediated cell cycle regulation did not appear to be involved in p53-mediated cellular quiescence (Supplementary Fig. 7G & H) (27,28).

DISCUSSION

The involvement of p53 in regulation of cellular quiescence has been documented in various experimental systems (10,29). Nonetheless, most of the previous studies were carried out in arbitrarily defined "quiescent" cells, a total cell population subjected to stress (5,20). Conceivably these studies encompassed cells that were forcefully arrested in other phases of the cell cycle, in particular, those in G1 phase that are not readily distinguishable from G0 cells by conventional cell cycle analysis approaches (30). Indeed, while the p53 transcriptional target p21 was shown to be critical for quiescence in some studies (31), we found that p21 was not involved in regulation of cellular quiescence, although it was upregulated in purified G0 cells. It is probable that the role of p21 in p53-mediated cellular quiescence reported in previous studies reflects its contribution to p53-induced G1 phase arrest (32). Thus, this discrepancy calls for more diligent investigation of the molecular mechanisms involved in the regulation of quiescence. In support, there is increasing evidence showing that G0 cells express distinct transcript profiles compared with cells in G1 phase (17). By taking advantage of a previously verified experimental system for visualizing G0 to G1 transition (17), we were able to faithfully isolate G0 and G1 cells through co-introducing mVenus-p27K$^-$ that cannot bind to CDK but is still prone to proteasomal degradation and mCherry-hCDT1(30/120) that is specifically expressed in G0 and G1 cells.

We focused on differentially expressed miRNAs between G0 and G1 cells, as a number of previous studies have shown that ablation of the miRNA processing enzyme Dicer promotes quiescence exit (33,34). Indeed, the list of miRNAs involved in cellular quiescence is rapidly expanding (33,35-39), but results from clearly defined putative G0 cells are currently lacking. Herein we identified miRNA-27b-3p and miRNA-455-3p as positive regulators of cellular quiescence through analysis of highly purified G0 and G1 cells. Mechanistic investigation revealed that both miRNA-27b-3p and miRNA-455-3p promoted p27 stabilization through sequestering Skp2-mediated degradation. Skp2 is known to be primarily responsible for degrading p27 in cells that proceed through S phase and afterwards (22,27), whereas its expression levels are low in cells during the G0 to G1 transition where p27

expression starts to be reduced (24). It is therefore likely that miRNA-27b-3p and miRNA-455-3p are mainly involved in promoting quiescence entry and maintenance.

Neither miRNA-27b-3p nor miRNA-455-3p directly targeted the transcript of p27. Instead, miRNA-27b-3p inhibited the expression of Cks1 that binds to Skp2 and prevents it from auto-ubiquitylation and degradation (24), whereas miRNA-455-3p targeted CAC1 that promotes CDK2 activity leading to increased phosphorylation of p27 at Thr187 which is necessary for polyubiquitination of p27 by Skp2. Therefore, albeit affecting p27 expression indirectly, these miRNAs act cooperatively to ensure that the molecular machinery that drives p27 degradation is under tight control. This interdependent relationship between miRNA-27b-3p and miRNA-455-3p in regulation of p27 also provides a mechanistic explanation as to why co-knockdown or co-overexpression of these miRNAs did not produce additive effects on p27 expression.

Interestingly, similar to the correlative relationship between miRNA-27b-3p and miRNA-455-3p expression levels, the transcript levels of the miRNA-27b-3p host gene *C9ORF3* and the miRNA-455-3p host gene *COL27A1* were positively correlated. These observations suggested that *C9ORF*3 and *COL27A1* were likely to be regulated by the same mechanism and we established this to be transcriptional regulation by p53. This not only identified *C9ORF3* along with miRNA-27b-3p and *COL27A1* together with miRNA-455-3p as novel transcriptional targets of p53, but also established these genes and their products as important components of p53-driven networks promoting cellular quiescence. However whether regulation of *C9ORF3* and *COL27A1* by p53 has other effects on cellular processes remains to be investigated.

Cellular quiescence is closely related to evasion of cancer cells to killing by systemic treatment, as most of available therapeutics primarily target proliferating cancer cells (40). Re-entry of quiescent cancer cells into the cell cycle plays an important role in relapse following initial tumour remission (15). Therefore, curative treatment of cancer requires therapies that either sustain the quiescent state or drive quiescent cells into the cell cycle to render them sensitive to induction of cell death (2,3). Accordingly, our results suggest that either promotion of miRNA-27b-3p and miRNA-455-3p expression to force cells to remain in the quiescent state permanently or inhibition of these miRNAs to

have quiescent cells re-enter the cell cycle is a testable approach for improving the therapeutic efficacy of systemic therapeutic agents.

In summary, we have shown in the study that p53 is a driver of quiescence in cancer cells through two interrelated miRNA pathways with potential implications for cancer treatment (Fig. 7G). Noticeably, although miRNA-27b-3p and miRNA-455-3p expression is primarily regulated by p53, they are detectable in *TP53*-null cells and those carrying mutant *TP53*, albeit at low levels. Considering that p53 inactivation through mutation or deletion occurs in >50% of human cancers (41), this suggests that unidentified mechanisms may be involved in regulation of the expression of miRNA-27b-3p and miRNA-455-3p that function independently of p53 to regulate cellular quiescence.

ACKNOWLEDGMENTS

The authors thank professor Toshio Kitamura (University of Tokyo, Tokyo, Japan) for the pMXs-IP-mVenus-p27K$^-$, pGag-pol-IRES-bs^r and pEnv-IRES-puro^r plasmids and Drs. Hiroyuki Miyoshi and Atsushi Miyawaki (RIKEN Brain Science Institute, Japan) for the mCherry-hCdt1(30/120)/pCSII-EF-MCS plasmids.

This work was supported by the National Health and Medical Research Council (NHMRC) (X. D. Zhang: APP1147271 and L. Jin: APP1099947) and the Cancer Council NSW (X. D. Zhang: RG 16-12). L. Jin is a recipient of Cancer Institute NSW Career Development Fellowship (LJ00397).

REFERENCE

1. Pantel K, Brakenhoff RH. Dissecting the metastatic cascade. Nat Rev Cancer **2004**;4:448-56
2. Aguirre-Ghiso JA. Models, mechanisms and clinical evidence for cancer dormancy. Nat Rev Cancer **2007**;7:834-46
3. Yeh AC, Ramaswamy S. Mechanisms of Cancer Cell Dormancy—Another Hallmark of Cancer? Cancer Research **2015**;75:5014-22
4. Hirata Y, Furuhashi K, Ishii H, Li HW, Pinho S, Ding L, *et al.* CD150(high) Bone Marrow Tregs Maintain Hematopoietic Stem Cell Quiescence and Immune Privilege via Adenosine. Cell stem cell **2018**;22:445-53.e5
5. Coller HA, Sang L, Roberts JM. A new description of cellular quiescence. PLoS Biol **2006**;4:e83
6. Scholzen T, Gerdes J. The Ki-67 protein: from the known and the unknown. J Cell Physiol **2000**;182:311-22
7. Besson A, Dowdy SF, Roberts JM. CDK Inhibitors: Cell Cycle Regulators and Beyond. Developmental Cell **2008**;14:159-69
8. Aguirre-Ghiso JA, Estrada Y, Liu D, Ossowski L. ERK(MAPK) activity as a determinant of tumor growth and dormancy; regulation by p38(SAPK). Cancer Res **2003**;63:1684-95
9. Kwon JS, Everetts NJ, Wang X, Wang W, Della Croce K, Xing J, *et al.* Controlling Depth of Cellular Quiescence by an Rb-E2F Network Switch. Cell reports **2017**;20:3223-35
10. Brien GL, Healy E, Jerman E, Conway E, Fadda E, O'Donovan D, *et al.* A chromatin-independent role of Polycomb-like 1 to stabilize p53 and promote cellular quiescence. Genes Dev **2015**;29:2231-43
11. Ganoth D, Bornstein G, Ko TK, Larsen B, Tyers M, Pagano M, *et al.* The cell-cycle regulatory protein Cks1 is required for SCF(Skp2)-mediated ubiquitinylation of p27. Nature cell biology **2001**;3:321-4
12. Kong Y, Nan K, Yin Y. Identification and characterization of CAC1 as a novel CDK2-associated cullin. Cell Cycle **2009**;8:3552-61
13. Montagnoli A, Fiore F, Eytan E, Carrano AC, Draetta GF, Hershko A, *et al.* Ubiquitination of p27 is regulated by Cdk-dependent phosphorylation and trimeric complex formation. Genes Dev **1999**;13:1181-9
14. Wang JY, Liu GZ, Wilmott JS, La T, Feng YC, Yari H, *et al.* Skp2-Mediated Stabilization of MTH1 Promotes Survival of Melanoma Cells upon Oxidative Stress. Cancer Research **2017**;77:6226
15. Xi Z, Yao M, Li Y, Xie C, Holst J, Liu T, *et al.* Guttiferone K impedes cell cycle re-entry of quiescent prostate cancer cells via stabilization of FBXW7 and subsequent c-MYC degradation. Cell Death Dis **2016**;7:e2252
16. Zhang YY, Tabataba H, Liu XY, Wang JY, Yan XG, Farrelly M, *et al.* ACTN4 regulates the stability of RIPK1 in melanoma. Oncogene **2018**
17. Oki T, Nishimura K, Kitaura J, Togami K, Maehara A, Izawa K, *et al.* A novel cell-cycle-indicator, mVenus-p27K-, identifies quiescent cells and visualizes G0-G1 transition. Sci Rep **2014**;4:4012
18. Nishitani H, Taraviras S, Lygerou Z, Nishimoto T. The human licensing factor for DNA replication Cdt1 accumulates in G1 and is destabilized after initiation of S-phase. J Biol Chem **2001**;276:44905-11
19. Hara T, Kamura T, Nakayama K, Oshikawa K, Hatakeyama S, Nakayama K. Degradation of p27(Kip1) at the G(0)-G(1) transition mediated by a Skp2-independent ubiquitination pathway. J Biol Chem **2001**;276:48937-43
20. Gos M, Miloszewska J, Swoboda P, Trembacz H, Skierski J, Janik P. Cellular quiescence induced by contact inhibition or serum withdrawal in C3H10T1/2 cells. Cell proliferation **2005**;38:107-16
21. Kim KH, Sederstrom JM. Assaying Cell Cycle Status Using Flow Cytometry. Curr Protoc Mol Biol **2015**;111:28 6 1-11

22. Kossatz U, Dietrich N, Zender L, Buer J, Manns MP, Malek NP. Skp2-dependent degradation of p27kip1 is essential for cell cycle progression. Genes Dev **2004**;18:2602-7
23. Tsvetkov LM, Yeh KH, Lee SJ, Sun H, Zhang H. p27(Kip1) ubiquitination and degradation is regulated by the SCF(Skp2) complex through phosphorylated Thr187 in p27. Current biology : CB **1999**;9:661-4
24. Bashir T, Dorrello NV, Amador V, Guardavaccaro D, Pagano M. Control of the SCF(Skp2-Cks1) ubiquitin ligase by the APC/C(Cdh1) ubiquitin ligase. Nature **2004**;428:190-3
25. Jin L, Hu WL, Jiang CC, Wang JX, Han CC, Chu P*, et al.* MicroRNA-149*, a p53-responsive microRNA, functions as an oncogenic regulator in human melanoma. Proc Natl Acad Sci U S A **2011**;108:15840-5
26. Suzuki HI, Yamagata K, Sugimoto K, Iwamoto T, Kato S, Miyazono K. Modulation of microRNA processing by p53. Nature **2009**;460:529-33
27. Starostina NG, Kipreos ET. Multiple degradation pathways regulate versatile CIP/KIP CDK inhibitors. Trends Cell Biol **2012**;22:33-41
28. Niculescu AB, Chen X, Smeets M, Hengst L, Prives C, Reed SI. Effects of p21(Cip1/Waf1) at Both the G(1)/S and the G(2)/M Cell Cycle Transitions: pRb Is a Critical Determinant in Blocking DNA Replication and in Preventing Endoreduplication. Molecular and Cellular Biology **1998**;18:1763-
29. Liu Y, Elf SE, Miyata Y, Sashida G, Liu Y, Huang G*, et al.* p53 Regulates Hematopoietic Stem Cell Quiescence. Cell stem cell **2009**;4:37-48
30. Denkert C, Furstenberg A, Daniel PT, Koch I, Kobel M, Weichert W*, et al.* Induction of G0/G1 cell cycle arrest in ovarian carcinoma cells by the anti-inflammatory drug NS-398, but not by COX-2-specific RNA interference. Oncogene **2003**;22:8653-61
31. Barr AR, Cooper S, Heldt FS, Butera F, Stoy H, Mansfeld J*, et al.* DNA damage during S-phase mediates the proliferation-quiescence decision in the subsequent G1 via p21 expression. Nat Commun **2017**;8:14728
32. Linke SP, Clarkin KC, Di Leonardo A, Tsou A, Wahl GM. A reversible, p53-dependent G0/G1 cell cycle arrest induced by ribonucleotide depletion in the absence of detectable DNA damage. Genes Dev **1996**;10:934-47
33. Cheung TH, Quach NL, Charville GW, Liu L, Park L, Edalati A*, et al.* Maintenance of muscle stem-cell quiescence by microRNA-489. Nature **2012**;482:524-8
34. Roche B, Arcangioli B, Martienssen RA. RNA interference is essential for cellular quiescence. Science **2016**;354
35. Almog N, Briggs C, Beheshti A, Ma L, Wilkie KP, Rietman E*, et al.* Transcriptional changes induced by the tumor dormancy-associated microRNA-190. Transcription **2013**;4:177-91
36. Galardi S, Mercatelli N, Giorda E, Massalini S, Frajese GV, Ciafre SA*, et al.* miR-221 and miR-222 expression affects the proliferation potential of human prostate carcinoma cell lines by targeting p27Kip1. J Biol Chem **2007**;282:23716-24
37. le Sage C, Nagel R, Egan DA, Schrier M, Mesman E, Mangiola A*, et al.* Regulation of the p27(Kip1) tumor suppressor by miR-221 and miR-222 promotes cancer cell proliferation. The EMBO journal **2007**;26:3699-708
38. Raffel S, Trumpp A. miR-126 Drives Quiescence and Self-Renewal in Leukemic Stem Cells. Cancer Cell **2016**;29:133-5
39. Sato T, Yamamoto T, Sehara-Fujisawa A. miR-195/497 induce postnatal quiescence of skeletal muscle stem cells. Nat Commun **2014**;5:4597
40. Kyle AH, Baker JH, Minchinton AI. Targeting quiescent tumor cells via oxygen and IGF-I supplementation. Cancer Res **2012**;72:801-9
41. Li T, Kon N, Jiang L, Tan M, Ludwig T, Zhao Y*, et al.* Tumor suppression in the absence of p53-mediated cell cycle arrest, apoptosis, and senescence. Cell **2012**;149:1269-83

FIGURE LEGENDS

Figure 1. MiR-27b-3p and miR-455-3p promote cellular quiescence in B16 cells. **A**, Representative flow cytometric plots of B16 cells stably expressing mCherry-hCdt1(30-120) and mVenus-p27K^{-} cultured under indicated conditions. Numbers represent percentage of quiescent cells. **B**, Quantitation of G0 cells in 3 independent experiments as shown in (A). **C**, Whole cell lysates from sorted G1 and G0 B16 cells were subjected to Western Blotting. **D**, Representative flow cytometric plots of unsorted and sorted mVenus-p27K^{-high}/mCherry-hCDT1(30/120)$^{+}$ B16 cells stained with an APC-conjugated anti-Ki67 antibody and propidium iodide. Ki67^{high} cells were gated as proliferating cells. Numbers represent percentage of proliferating cells. **E**, Representative flow cytometric plots of unsorted (left), sorted mVenus-p27K^{-low} mCherry-hCDT1(30/120)$^{+}$ (middle) and mVenus-p27K^{-high} mCherry-hCDT1(30/120)$^{+}$ (right) B16 cells stained with Hoechst-33342 and Pyronin Y. Pyronin Y^{high} Hoechst-33342^{low} and Pyronin Y^{low} Hoechst-33342 ^{low} cells were gated as G1 and G0 cells, respectively. Numbers represent percentage of cells in G1 (higher) or G0 (lower). **F**, Total RNA from sorted G1 and G0 B16 cells were subjected to qPCR analysis. **G**, Total RNA from B16 cells transfected with indicated RNA oligonucleotides were subject to qPCR analysis. **H**, B16 cells transfected with indicated RNA oligonucleotides were cultured with or without serum starvation. Twenty-four hours later, cells were subjected to Hoechst-33342 and Pyronin Y double staining followed by analysis using cytometry. **I**, Total RNA from B16 cells transfected with indicated microRNA mimics were subject to qPCR analysis. **J**, Representative flow cytometric plots of B16 cells transfected with indicated microRNA mimics cultured with or without serum starvation. Twenty-four hours later, cells were subjected to Hoechst-33342 and Pyronin Y double staining followed by analysis using cytometry.
Data shown are either representative (A, C, D and E) or mean ± SEM (B, F, G, H, I and J) of three individual experiments. *, $P<0.05$, **, $P<0.01$, ***, $P<0.001$, Student's *t*-test.

Figure 2. MiR-27b-3p and miR-455-3p are up-regulated in quiescent cells and promote cellular quiescence in various human cancer cell lines. **A,** Total RNA from Mel-RM, U2OS, A549 and HCT116 cells cultured with or without serum starvation for 36 hours followed by serum replenishment for another 12 hours were subjected to qPCR analysis. **B,** Mel-RM (left) and A549 (right) cells

transfected with indicated RNA oligonucleotides were cultured with or without serum starvation. Twenty-four hours later, cells were subjected to Hoechst-33342 and Pyronin Y double staining followed by analysis using cytometry. **C,** Whole cell lysates from Mel-RM cells transfected with indicated RNA oligonucleotides cultured with or without serum starvation were subject to Western blotting. **D,** Mel-RM cells transfected with indicated RNA oligonucleotides cultured with or without serum starvation were subjected to staining with an APC-conjugated anti-Ki67 antibody and analysis using flow cytometry. **E,** Mel-RM (left) and A549 (right) cells transfected with indicated anti-miRNA oligonucleotides were cultured with or without serum starvation. Twenty-four hours later, cells were subjected to Hoechst-33342 and Pyronin Y double staining followed by analysis using cytometry. **F,** Whole cell lysates from Mel-RM cells transfected with indicated anti-miRNA oligonucleotides cultured with or without serum starvation were subject to Western blotting. **G,** Mel-RM cells transfected with indicated anti-miRNA oligonucleotides cultured with or without serum starvation were subjected to staining with an APC-conjugated anti-Ki67 antibody and analysis using flow cytometry. **H,** Viable Mel-RM cells were counted in an automated cell counter 24, 48 and 72 hours after transfection with indicated miRNA mimics. **I,** Mel-RM cells transfected with indicated miRNA mimics were subjected to clonogenic assay. ColonyArea was quantitated using ImageJ-plugin; ColonyArea in cells introduced with control (Ctrl) mimics was arbitrarily designated as 1. Scale bar, 1 cm. **J,** Representative photographs (left) and growth curves (right) of tumour xenografts of Mel-RM cells with or without introduction of miR-27b-3p or miR-455-3p mimics. n=6 mice per group.

Data shown are either representative (C, F, I (lower) and J (left)) or mean ± SEM (A, B, D, E, G, H, I (upper) andJ (right)) of three individual experiments. *, $P<0.05$, **, $P<0.01$, ***, $P<0.001$, Student's *t*-test.

Figure 3. MiR-27b-3p and miR-455-3p promote p27 stabilization through downregulating Skp2 and promoting its phosphorylation at Thr187, respectively. **A,** Whole cell lysates from Mel-RM cells transfected with indicated anti-miRNA oligonucleotides treated with cycloheximide (CHX; 5μg/ml) for indicated periods were subjected to Western Blotting. Quantitation of p27 relative to GAPDH expression is also shown (right). **B,** Immunoprecipitates with an antibody against Flag from whole cell

lysates of A549 cells transfected with indicated anti-miRNA oligonucleotides and plasmids were subjected to Western blotting. **C,** Whole cell lysates from Mel-RM cells transfected with indicated anti-miRNA oligonucleotides treated with cycloheximide (CHX; 5μg/ml) for indicated periods were subjected to Western Blotting. Quantitation of Skp2 relative to GAPDH expression is also shown (right). **D & E,** Whole cell lysates from Mel-RM cells co-transfected with indicated anti-miRNA oligonucleotides and siRNAs with or without treatment with cycloheximide (CHX; 5μg/ml) for indicated periods were subjected to Western blotting. Quantitation of p27 relative to GAPDH expression is also shown (right). **F & G,** Whole cell lysates from Mel-RM cells transfected with indicated anti-miRNA (F) or RNA (G) oligonucleotides were subjected to Western Blotting. Numbers represent quantitation of p27 phosphorylated at Thr187 relative to total p27 expression. **H**, Whole cell lysates from Mel-RM cells co-transfected with indicated anti-miRNA oligonucleotides and plasmids with or without treatment with cycloheximide (CHX; 5μg/ml) for indicated periods were subjected to Western blotting. Quantitation of Flag relative to GAPDH expression is also shown (right).

Data shown are either representative (A (left), B, C (left), D (left), E (left), F, G and H (left)) or mean ± SEM (A (right), C (right), D (right), E (right) and H (right)) of three individual experiments. *, $P<0.05$, **, $P<0.01$, ***, $P<0.001$, Student's *t*-test.

Figure 4. MiR-27b-3p suppresses Skp2 expression through targeting CKS1, whereas miR-455-3p inhibits p27 phosphorylation through targeting CAC1. **A,** Luciferase reporter activity measured in Mel-RM (left) and A549 (right) cells after co-transfection with indicated reporter constructs and miRNA mimics. **B,** Luciferase reporter activity measured in Mel-RM (left) and A549 (right) cells after co-transfecting cells with indicated reporter constructs and anti-miRNA oligonucleotides. **C** & **D**, Whole cell lysates from Mel-RM and A549 cells transfected with indicated miRNA mimics (C) or anti-miRNA oligonucleotides (D) were subjected to Western Blotting. **E**, Whole cell lysates from Mel-RM cells co-transfected with indicated miRNA mimics and cDNAs were subjected to Western blotting. **F**, Whole cell lysates from Mel-RM cells co-transfected with indicated anti-miRNA oligonucleotides and siRNAs were subjected to Western Blotting. **G** & **H**, Mel-RM (left) and A549 (right) cells were co-transfected with indicated reporter constructs and miRNA mimics (G) or anti-

miRNA oligonucleotides (H). Twenty-four hours later, reporter activity was measured using luciferase assays. **I & J**, Whole cell lysates from Mel-RM and A549 cells transfected with indicated miRNA mimics (I) or anti-miRNA oligonucleotides (J) were subjected to Western Blotting. **K,** Whole cell lysates from Mel-RM cells co-transfected with indicated miRNA mimics and cDNAs were subjected to Western Blotting. **L,** Whole cell lysates from Mel-RM cells co-transfected with indicated anti-miRNA oligonucleotides and siRNAs were subjected to Western Blotting.

Data shown are either representative (C, D, E, F, I, J, K and L) or mean ± SEM (A, B, G and H) of three individual experiments. *, $P<0.05$, **, $P<0.01$, ***, $P<0.001$, Student's *t*-test.

Figure 5. Co-regulation of miRNA-27b-3p and miRNA-455-3p and their host genes. **A,** Two-sided Pearson's correlation was employed to analyze the correlation between C9ORF3 and COL27A1 mRNA levels in data from 35763 various cancer patient samples acquired from the R2 Genomics Analysis and Visualization Platform. **B,** Regression analysis showing the positive correlation between miR-27b-3p and miR-455-3p levels in a cell line panel comprised of Mel-RM, Sk-Mel-28, A375, U2OS, A549, MCF7, HeLa, WiDr, HT-29 and HCT116. **C,** Total RNA from Mel-RM cells transfected with indicated siRNAs were subjected to qPCR analysis of miR-27b-3p (upper) and C9ORF3 (lower) mRNA expression. **D,** Total RNA from Mel-RM cells transfected with indicated siRNAs were subjected to qPCR analysis of miR-455-3p (upper) and COL27A1 (lower) mRNA expression. **E**, Total RNA from Mel-RM cells cultured with or without serum starvation for 36 hours followed by serum replenishment for another 12 hours were subjected to qPCR analysis C9ORF3 and COL27A1 mRNA expression. **F**, Mel-RM cells transfected with indicated siRNAs cultured with or without serum starvation were subjected to Hoechst-33342 and Pyronin Y double staining followed by analysis using cytometry.

Data shown are mean ± SEM (C, D, E and F) of three individual experiments. **, $P<0.01$, ***, $P<0.001$, Student's *t*-test.

Figure 6. p53 transcriptionally regulates miRNA-27b-3p and miRNA-455-3p. **A & B**, Luciferase reporter activity measured in Mel-RM cells transfected with indicated *C9ORF3* (A) or *COL27A1* (B)

promoter reporter constructs as illustrated (upper) cultured with or without serum starvation. **C** & **D**, Luciferase reporter activity measured in Mel-RM cells transfected with pGL3-C9ORF3-(-250/+100) (C) or pGL3-COL27A1-(-1000/+100) (D) cultured with or without serum starvation followed by serum replenishment. S: serum; SS: serum starvation; SSR: Serum replenishment. **E & F,** Luciferase reporter activity measured in Mel-RM cells transfected with wild-type or mutant (lacking p53 binding sites) *C9ORF3* (E) or *COL27A1* (F) reporter constructs as illustrated (upper) cultured with or without serum starvation. **G,** Luciferase reporter activity measured in Mel-RM cells transfected with indicated cDNAs and promoter reporter constructs. 53ΔTA: p53 mutant lacking the transactivation domain. **H & I,** Luciferase reporter activity measured in Mel-RM cells transfected with indicated promoter reporter constructs with or without co-introduction of indicated siRNA (H) or treatment with PTFα (40 nmol/ml). **J,** Mel-RM (left) and A549 (right) cells cultured with or without serum starvation for 36 hours were subjected to chromatin immunoprecipitation (ChIP). **K** & **L,** Total RNA from Mel-RM cells transfected with indicated siRNAs (K) or treated with PTFα (40 nmol/ml) (L) were subjected to qPCR analysis of pir-miR-27b-3p and pri-miR-455-3p. SS: serum starvation. **M,** Total RNA from Mel-RM cells transfected with indicated cDNAs cultured with or without serum starvation were subjected to qPCR analysis of pir-miR-27b-3p (upper) and pri-miR-455-3p (lower).

Data shown are either representative (J) or mean ± SEM (A, B, C, D, E, F, G, H, I, K, L and M) of three individual experiments. *, $P<0.05$, **, $P<0.01$, ***, $P<0.001$, Student's *t*-test.

Figure 7. p53 drives cellular quiescence through miRNA-27b-3p and miRNA-455-3p. **A & B,** Mel-RM cells co-transfected with indicated miRNA mimics and siRNAs (A) or anti-miRNA oligonucleotides and cDNAs (B) were cultured with serum starvation. Twenty-four later, cells were subjected to Hoechst-33342 and Pyronin Y staining followed by analysis using flow cytometry. **C & D**, Whole cell lysates from Mel-RM cells co-transfected with indicated miRNA mimics and siRNA (C) or anti-miRNA oligonucleotides and cDNA (D) were subjected to Western Blotting. **E & F**, Mel-RM cells co-transfected with p53 cDNA and p27 siRNAs (E) or p27 cDNA and p53 siRNAs (F) were cultured with serum starvation. Twenty-four later, cells were subjected to Hoechst-33342 and Pyronin

Y staining followed by analysis using flow cytometry. **G,** A schematic illustration of the identified p53-responsive microRNA network that promotes cellular quiescence.

Data shown are either representative (C and D) or mean ± SEM (A, B, E and F) of three individual experiments. *, $P<0.05$, **, $P<0.01$, Student's *t*-test.

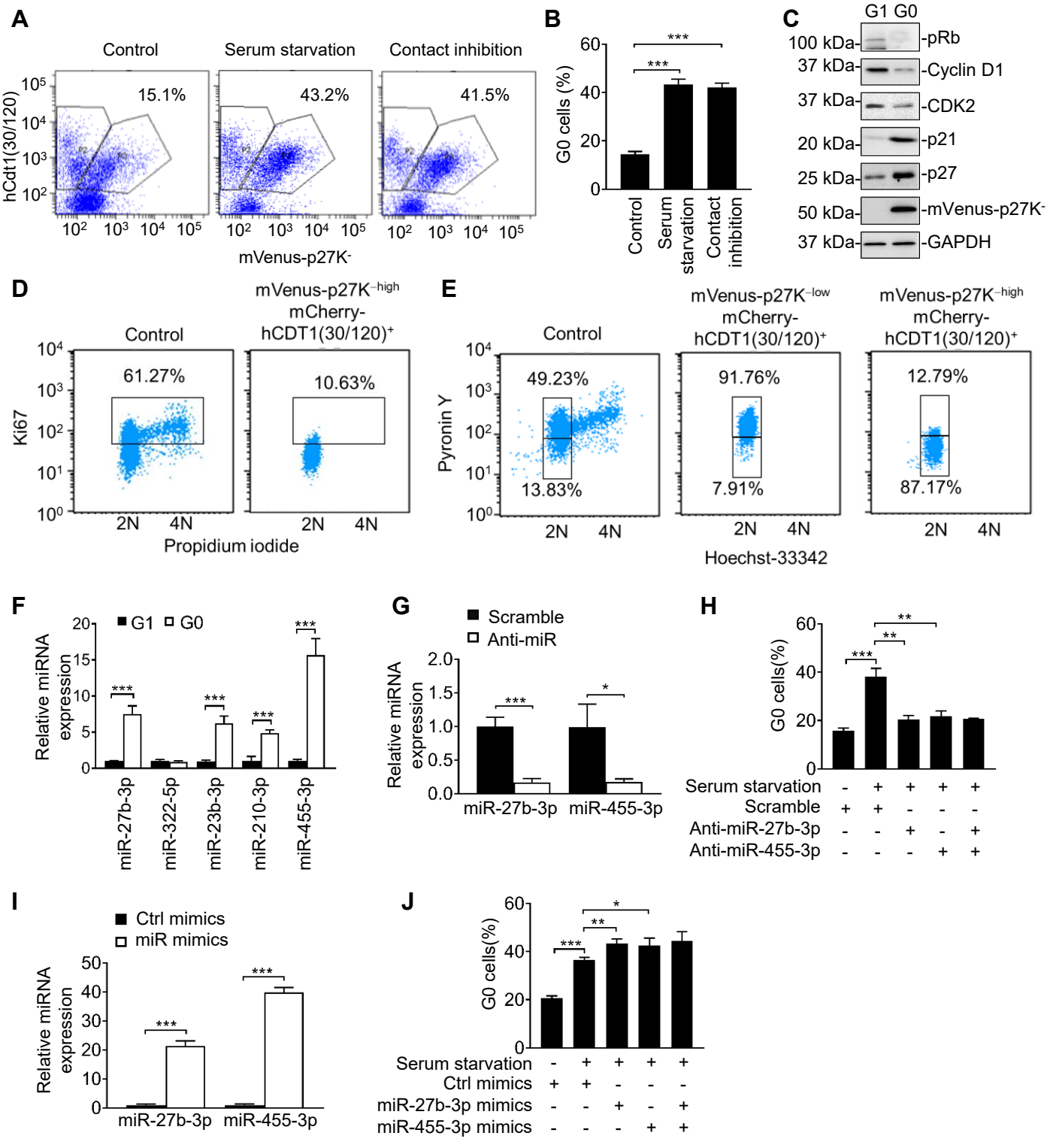

Figure 1

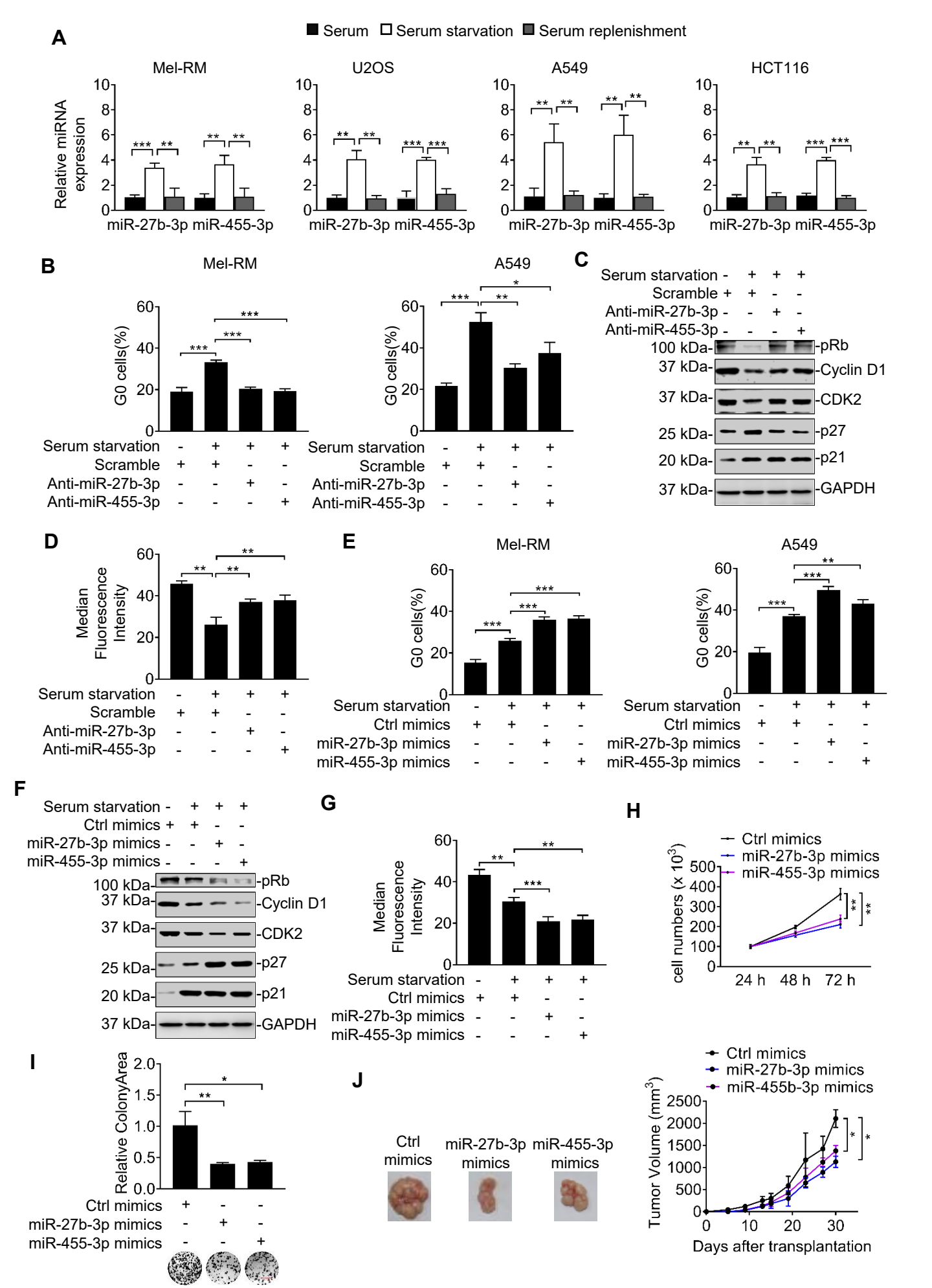

Figure 2

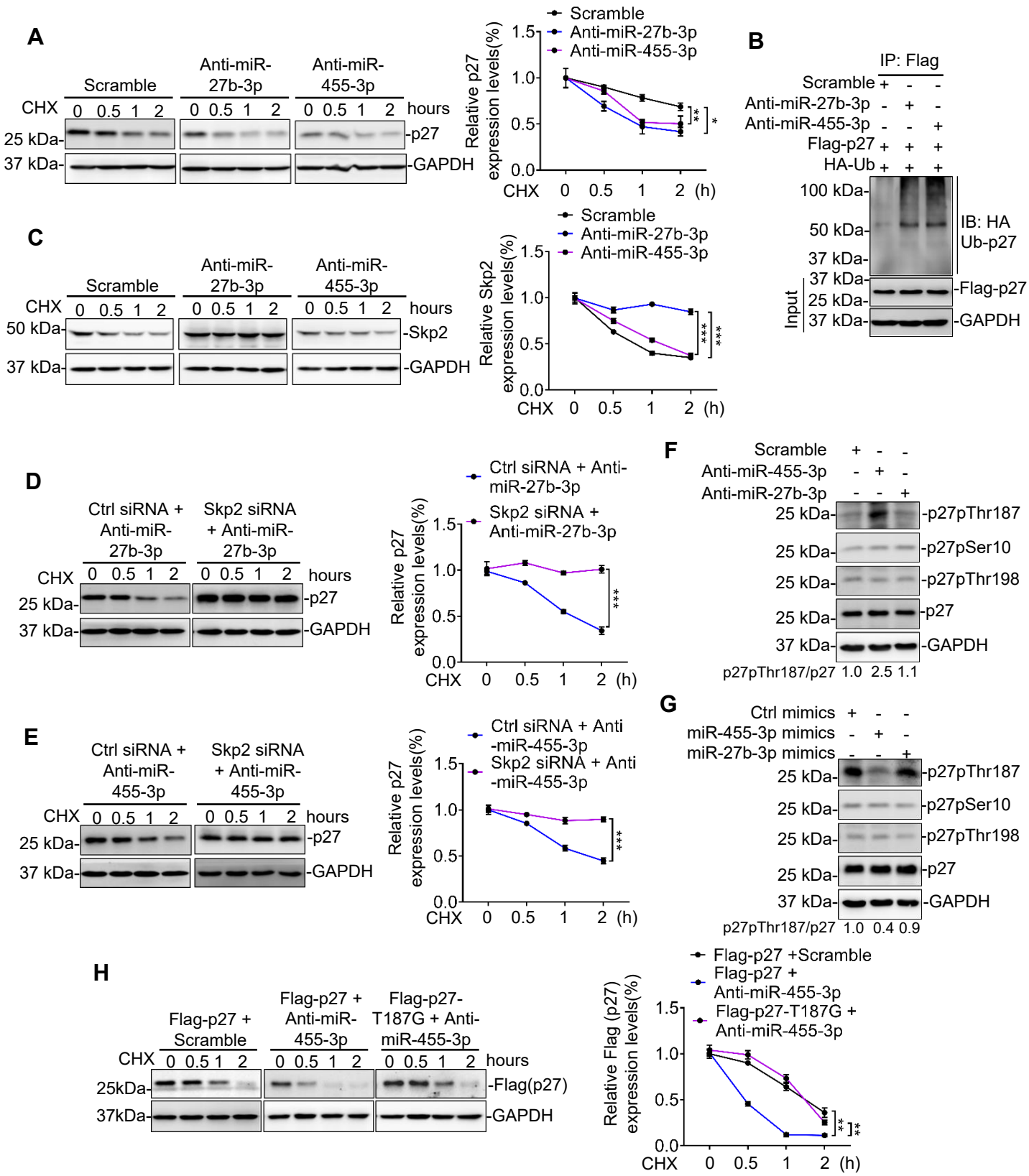

Figure 3

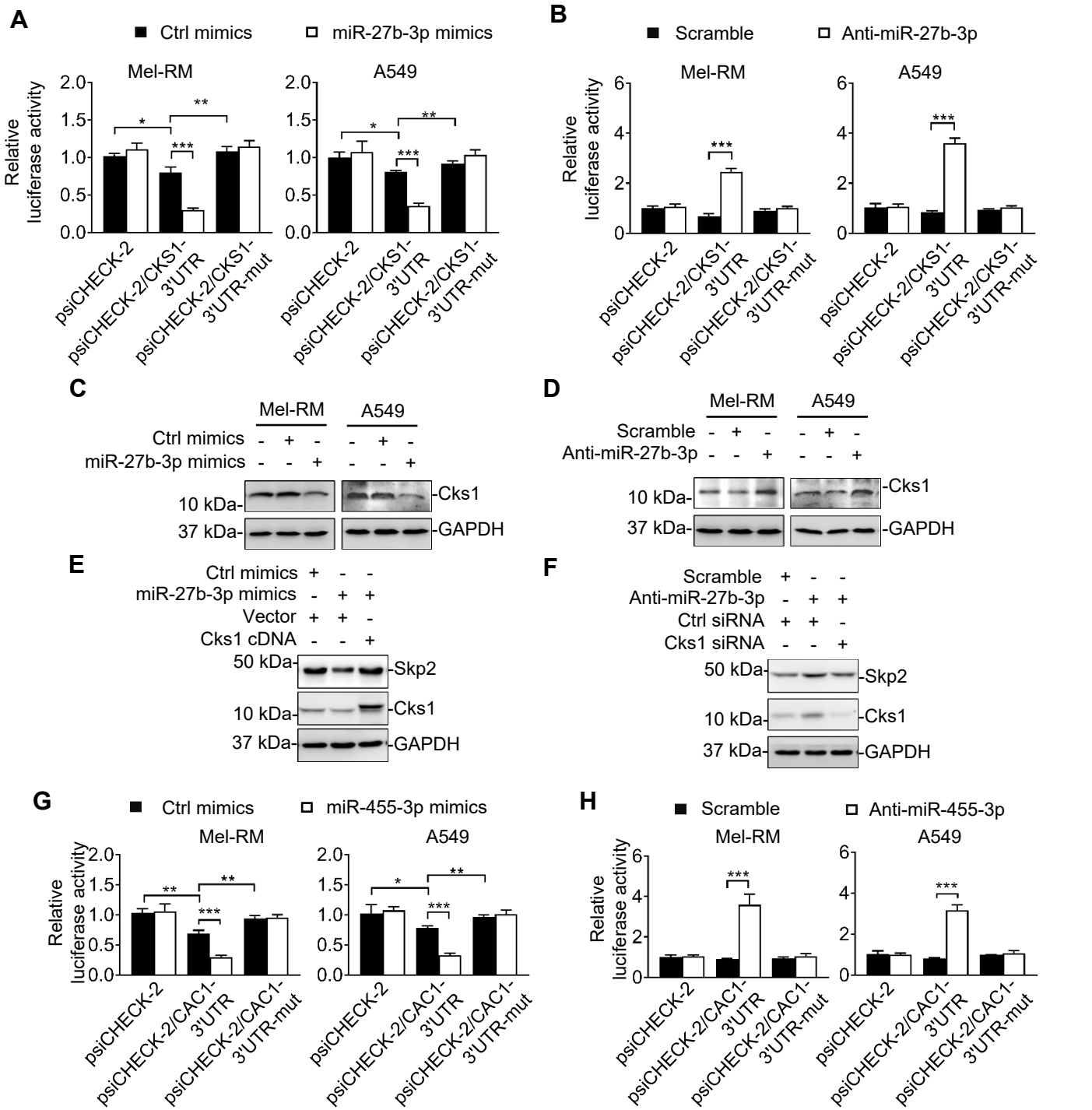

Figure 4

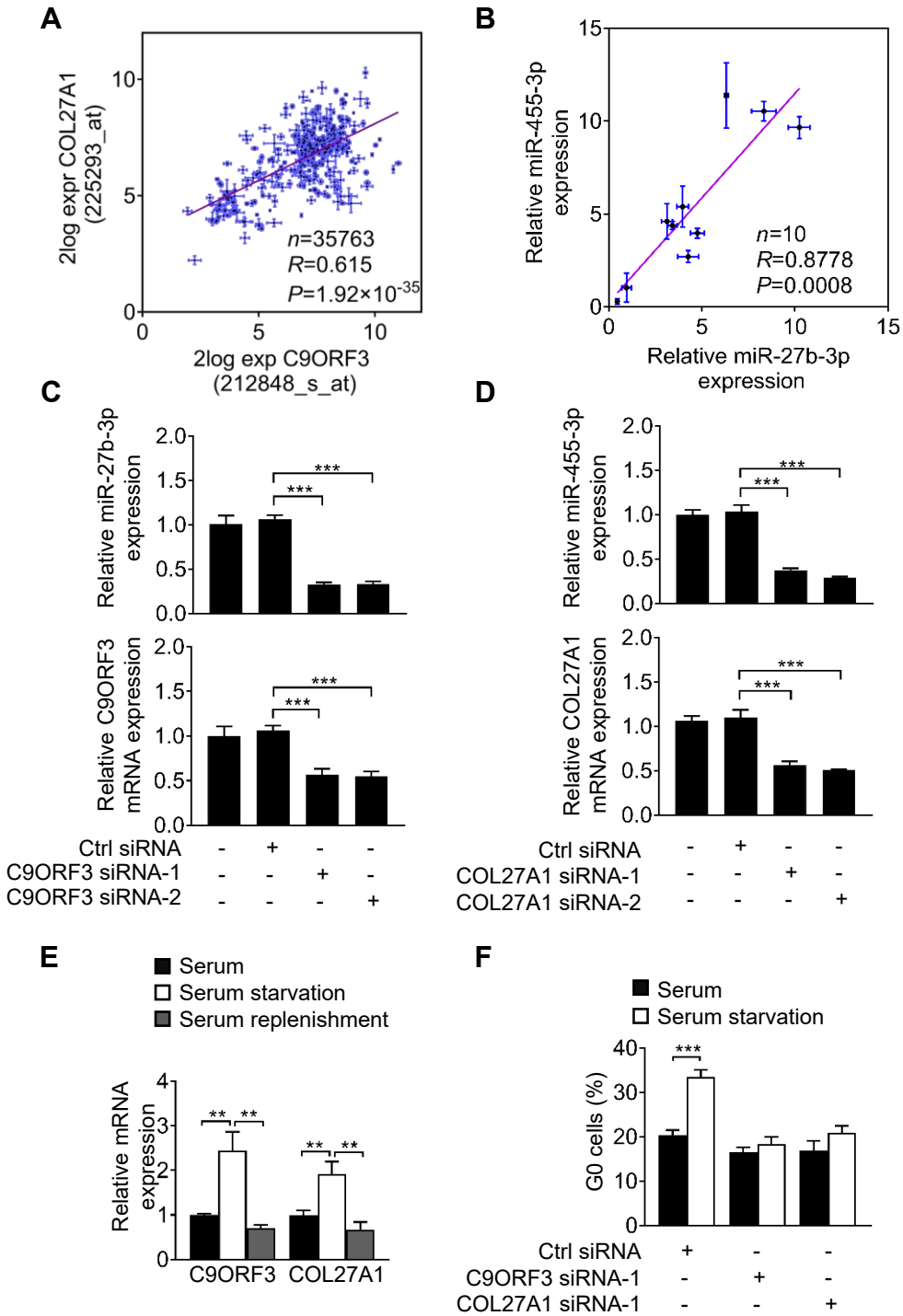

Figure 5

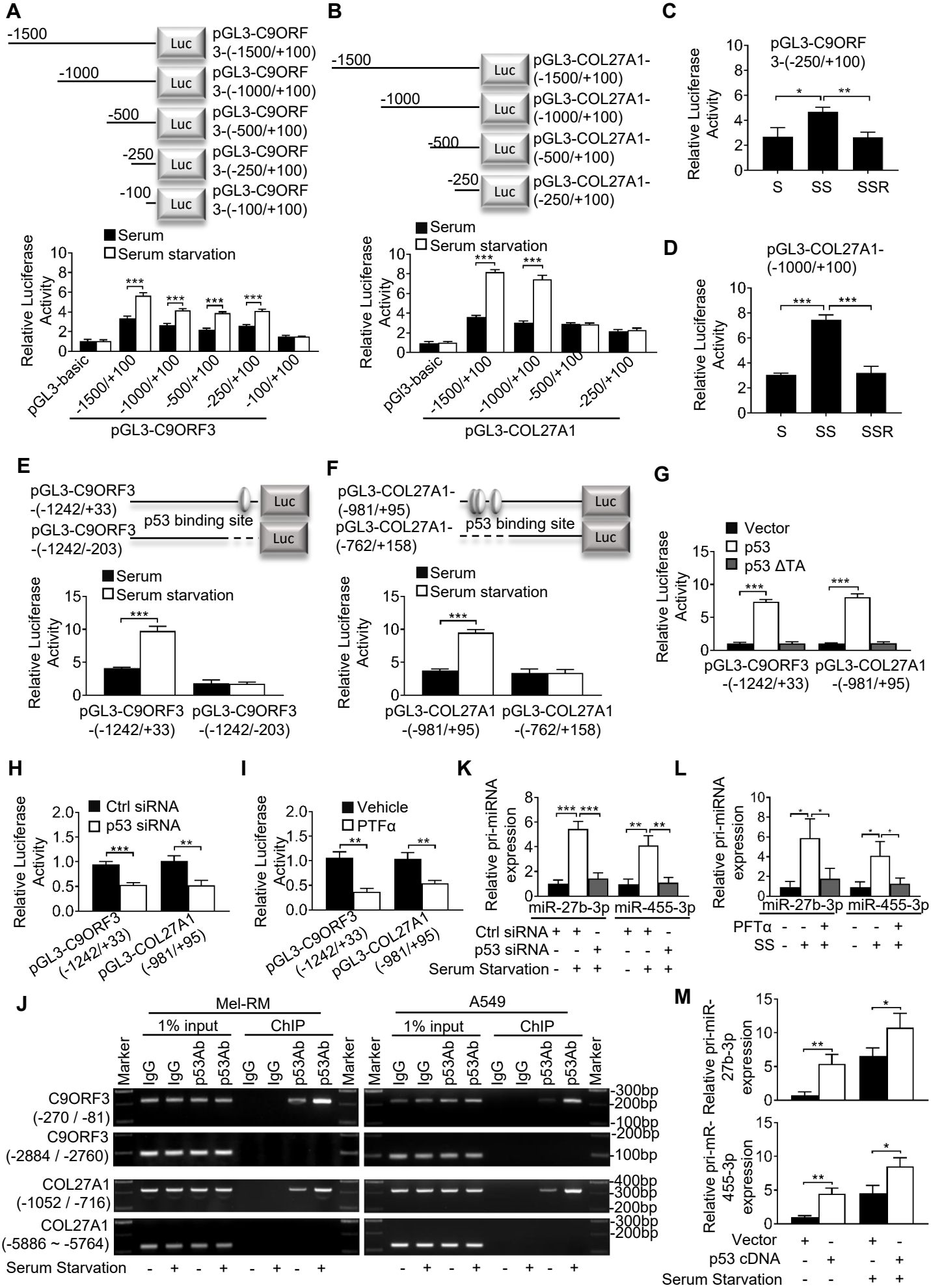

Figure 6

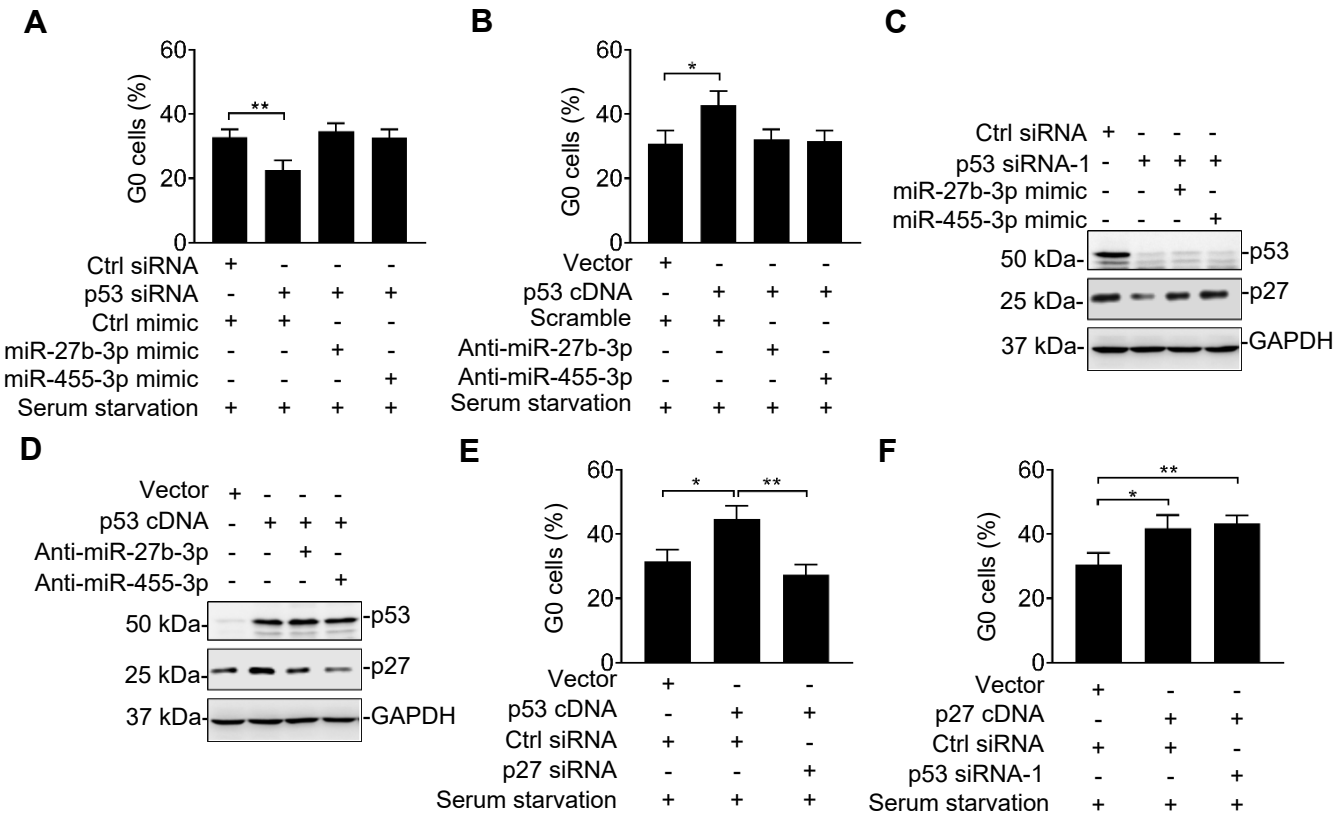

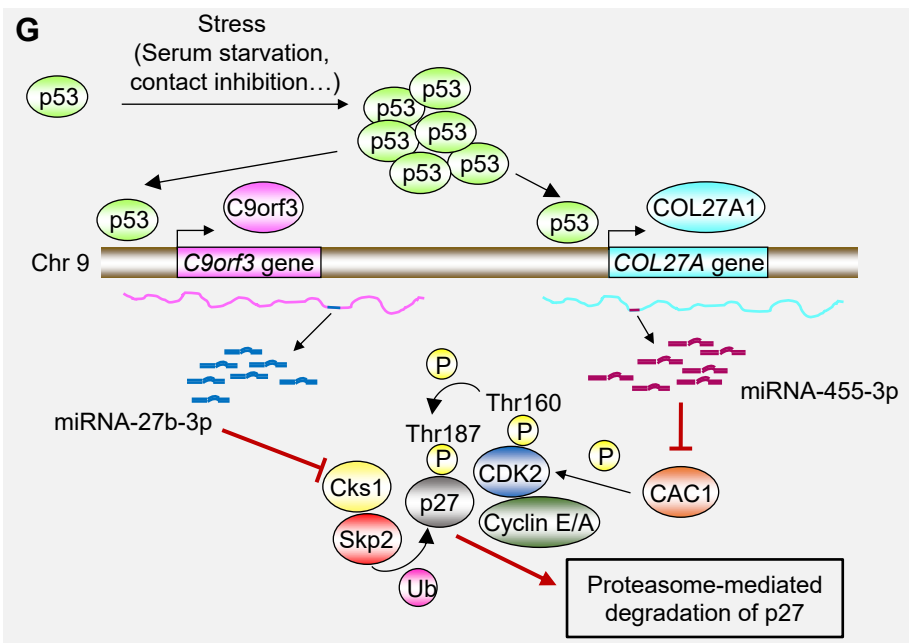

Figure 7

AACR American Association for Cancer Research

Cancer Research

The Journal of Cancer Research (1916–1930) | The American Journal of Cancer (1931–1940)

A p53-responsive microRNA network promotes cancer cell quiescence

Ting La, Guang Zhi Liu, Margaret Farrelly, et al.

Cancer Res Published OnlineFirst October 9, 2018.